RSC Medicinal Chemistry

ROYAL SOCIETY OF CHEMISTRY

RESEARCH ARTICLE

View Article Online
View Journal

Cite this: DOI: 10.1039/c9md00390h

Hydrocortisone/cyclodextrin complex electrospun nanofibers for a fast-dissolving oral drug delivery system†

Asli Celebioglu * and Tamer Uyar *

The electrospinning of hydrocortisone/cyclodextrin complex nanofibers was performed in order to develop a fast-dissolving oral drug delivery system. Hydrocortisone is a water-insoluble hydrophobic drug, yet, the water solubility of hydrocortisone was significantly enhanced by inclusion complexation with hydroxypropyl-beta-cyclodextrin (HP-β-CyD). In this study, hydrocortisone/HP-β-CyD complexes were prepared in aqueous solutions having molar ratios of 1/1, 1/1.5 and 1/2 (hydrocortisone/HP-β-CyD). Highly concentrated aqueous solutions of HP-β-CyD (180%, w/v) were used for hydrocortisone/HP-β-CyD systems (1/1, 1/1.5 and 1/2) in order to perform electrospinning without the use of an additional polymer matrix. The turbidity of hydrocortisone/HP-β-CyD (1/1 and 1/1.5) aqueous solutions indicated the presence of some uncomplexed crystals of hydrocortisone whereas the aqueous solution of hydrocortisone/HP-β-CyD (1/2) was homogeneous indicating that hydrocortisone becomes totally water-soluble by inclusion complexation with HP-β-CyD. Nonetheless, the electrospinning of hydrocortisone/HP-β-CyD systems (1/1, 1/1.5 and 1/2) successfully yielded defect-free uniform nanofibrous structures. Moreover, the electrospinning process was quite efficient that hydrocortisone was completely preserved without any loss yielding hydrocortisone/HP-β-CyD nanofibers having the initial molar ratios (1/1, 1/1.5 and 1/2). The structural and thermal characterization of the hydrocortisone/HP-β-CyD nanofibers revealed that hydrocortisone was totally inclusion complexed with HP-β-CyD and was in the amorphous state in hydrocortisone/HP-β-CyD (1/2) nanofibers whereas some uncomplexed crystalline hydrocortisone was present in hydrocortisone/HP-β-CyD (1/1 and 1/1.5) nanofibers. Nevertheless, hydrocortisone/HP-β-CyD (1/1, 1/1.5 and 1/2) complex aqueous systems were electrospun in the form of nanofibrous webs having a free-standing and flexible nature. The hydrocortisone/HP-β-CyD (1/1, 1/1.5 and 1/2) nanofibrous webs have shown fast-dissolving behavior in water or when they were in contact with artificial saliva. Yet, the hydrocortisone/HP-β-CyD (1/2) nanofibrous web dissolved more quickly than the hydrocortisone/HP-β-CyD (1/1 and 1/1.5) nanofibrous webs due to the full inclusion complexation and the amorphous state of hydrocortisone in this sample. In short, the results suggest that polymer-free electrospun nanofibrous webs produced from hydrocortisone/HP-β-CyD could be quite applicable for fast-dissolving oral drug delivery systems.

Received 6th August 2019,
Accepted 7th October 2019

DOI: 10.1039/c9md00390h

rsc.li/medchem

Introduction

Fast-dissolving oral drug delivery systems are gaining more and more interest in the pharmaceutical industry.[1–5] These fast-dissolving oral drug delivery systems are mostly in the form of tablets and films/strips which either dissolve or disintegrate in the mouth very rapidly without the need of any water for swallowing the drugs.[1–7] Recently, electrospinning of nanofibrous webs incorporating active pharmaceutical ingredients (APIs) was shown to be a very favourable approach for the development of fast-dissolving drug delivery systems.[8–24] The electrospun nanofibrous webs made of hydrophilic materials can readily dissolve or disintegrate due to their very large surface area and highly porous structure.[16–21] Electrospinning can be an alternative to freeze drying which has potential to continuously produce solid nanofibrous formulations incorporating APIs with very high encapsulation efficiency.[22] Moreover, due to the excellent drying effect of the electrospinning process, API loaded nanofibrous webs can be used as they are if the electrospinning solutions are formulated for the final dosage of APIs or they can be continuously electrospun onto a water-soluble matrix to obtain a double-layered structure, which can be cut into orally fast-dissolving webs as finished dosage forms by the continuous process.[23,24]

Department of Fiber Science & Apparel Design, College of Human Ecology, Cornell University, Ithaca, NY, 14853, USA. E-mail: ac2873@cornell.edu, tu46@cornell.edu

† Electronic supplementary information (ESI) available. See DOI: 10.1039/c9md00390h

The incorporation of APIs in the electrospun fiber matrix can be performed either by solution electrospinning in which the carrier matrix and API are dissolved or dispersed in a common solution[21] or with a solvent-free approach by melt electrospinning.[25,26] The solution electrospinning approach is an easy and versatile process and more common compared to melt electrospinning to incorporate APIs into the nanofiber matrix, since the solution electrospinning process does not require high temperature and it is typically performed at room temperature. The melt electrospinning approach is very limited since there are only a few biopolymers that can be melt electrospun and since high temperature is required for melting the polymeric matrix, there is also a possibility of thermal degradation or evaporation of APIs during the melt electrospinning process. The solution electrospinning process also offers different nozzle setups including single nozzles,[8,14,19] multiple nozzles,[27] and core–shell nozzles,[18,20,28] and nozzle-less electrospinning is possible as well.[29]

Hydrophilic water-soluble polymeric matrices (*e.g.*, polyvinylpyrrolidone (PVP),[9,13,17,30,31] gelatin,[16,19,32] poly(vinyl alcohol) (PVA),[33] and chitosan/pullulan[34]) are chosen for the electrospinning of nanofibrous webs and the incorporation of APIs mostly results in amorphous dispersion within the polymeric nanofiber matrix after electrospinning.[9,10,12,17,35] The very large surface area and highly porous structure along with the amorphous state of APIs make these nanofibrous webs suitable for fast-dissolving oral drug delivery systems. Very recently, it has been shown that polymer-free fast-dissolving oral drug delivery systems can be developed by electrospinning of nanofibers from cyclodextrin inclusion complexes with drugs (*i.e.*, sulfisoxazole,[8] paracetamol,[14] spironolactone,[36] diclofenac sodium,[15] voriconazole,[22] and ibuprofen[37]) without using any polymeric matrix. Cyclodextrins (CyDs) are already being used in drug formulations since hydrophobic APIs become water-soluble by inclusion complexation with CyDs. Moreover, such API/CyD inclusion complex systems can also enhance the bioavailability and stability of APIs.[38–40] In addition, the electrospinning of nanofibers from aqueous solutions of CyD inclusion complexes with APIs has another advantage where it is possible to use only water for the electrospinning without the need of a polymeric carrier and without using organic solvents.[8,14,22] On the other hand, when biopolymers are used as carrier nanofiber matrices for encapsulating the APIs, mostly ethanol or some other acidic or organic solvent mixtures are used for the electrospinning solution in order to dissolve the polymer matrix and hydrophobic APIs, so, the presence of a residual toxic solvent could raise safety concerns for such systems.[9,13,17,19,30–34]

CyDs are produced from enzymatically hydrolyzed starch by the action of cyclodextrin glucosyltransferase and they are classified as cyclic oligosaccharides having a doughnut-shaped molecular structure. CyDs can form inclusion complexes with a variety of hydrophobic molecules including APIs within their truncated cone-shaped hydrophobic cavity due to hydrophobic interactions. CyDs are water-soluble, in particular, modified CyDs (*e.g.*, hydroxypropylated-CyD, methylated-CyD and sulfobutylated-CyD) are highly water-soluble compared to native CyDs (*i.e.*, α-CyD, β-CyD and γ-CyD).[41] Therefore, inclusion complexation of hydrophobic APIs with CyDs significantly improves their water-solubility and increase their bioavailability.[41,42]

The electrospinning of API/CyD inclusion complex formulations would yield nanofibrous webs with a fast-dissolving character and such electrospun nanofibrous webs would be quite suitable for designing fast-dissolving oral drug delivery systems for pharmaceutical products.[43] For instance, electrospinning of polymeric nanofibers incorporating API/CyD inclusion complexes was performed for fast-dissolving drug delivery purposes.[19,43] Moreover, electrospinning of API/CyD inclusion complex systems without using any polymeric matrix would provide more advantages for the development of fast-dissolving oral drug delivery systems.[8,14,15,22,36,37] For instance, CyDs are highly water-soluble compared to polymeric matrices, hence, with CyDs being a fiber matrix and inclusion complex host, nanofibers solely electrospun from API/CyD inclusion complexes would dissolve instantly in the oral cavity without the need of water and provide enhanced solubility to APIs by inclusion complexation. Also, by polymer-free electrospinning of API/CyD systems,[8,37] much higher API loadings are possible if needed for the finished dosage forms. The formulation of poorly water-soluble APIs into orally fast-dissolving tablets/films is quite a challenge since the volume of saliva in the oral cavity is very low when compared to that of the gastric liquid. Hence, most of the currently marketed orally fast-dissolving drugs are either formulated with salt forms of APIs or they are simply formulated with the choice of APIs having high water-solubility.[44,45] Therefore, polymer-free electrospun nanofibrous webs of CyD inclusion complexes with poorly water-soluble APIs would have very fast-dissolution in the oral cavity due to the very large surface area and highly porous structure of the API/CyD nanofibrous webs along with the very high water-solubility of CyDs and enhanced water-solubility of APIs by CyD inclusion complexation.[8,37]

In this study, we have chosen hydrocortisone as a model API for the electrospinning of polymer-free nanofibrous webs of a hydrocortisone/CyD inclusion complex for the development of orally fast-dissolving drug delivery systems. Hydrocortisone, a corticosteroid, is extensively used in therapy due to its broad range of anti-inflammatory and immunosuppressive effects. However, hydrocortisone is a water-insoluble hydrophobic drug molecule that suffers from low bioavailability, nonetheless, the water solubility of hydrocortisone can be significantly enhanced by CyD inclusion complexes.[46–49] For instance, the use of CyDs is considered for the oral disease treatment of hydrocortisone,[50] formulation of aqueous ophthalmic solutions of hydrocortisone,[51] and in oral paediatric hydrocortisone solution.[48] Electrospinning of polymeric nanofibers incorporating hydrocortisone has also been reported for skin wound healing[52–55] and controlled drug delivery purposes.[56] Yet, to the best of our knowledge, there is

no study related to fast-dissolving electrospun nanofibrous webs incorporating hydrocortisone. More importantly, this is the first report summarizing our effort to develop an orally fast-dissolving hydrocortisone delivery system based on polymer-free electrospun nanofibrous webs of hydrocortisone/CyD inclusion complexes.

Experimental

Materials

Hydroxypropyl-beta-cyclodextrin (HP-β-CyD, Cavasol W7 HP, DS: ~0.9) was a free-sample donated by Wacker Chemie AG (USA). Hydrocortisone (98%, Alfa Aesar), deuterated dimethylsulfoxide (d6-DMSO, 99.8%, Cambridge Isotope), sodium chloride (NaCl, >99%, Sigma Aldrich), potassium phosphate monobasic (KH_2PO_4, ≥99.0%, Fisher Chemical), sodium phosphate dibasic heptahydrate (Na_2HPO_4, 98.0–102.0%, Fisher Chemical) and *o*-phosphoric acid (85% (HPLC), Fisher Chemical) were obtained commercially. All chemicals were used without additional purification. High-quality distilled water was supplied from a Millipore Milli-Q ultrapure water system.

Electrospinning of nanofibers

Clear hydroxypropyl-beta-cyclodextrin (HP-β-CyD) solutions were prepared in distilled water with 180% (w/v) solid concentration. Hydrocortisone was subsequently added to the clear HP-β-CyD solutions to attain 1/0.5, 1/1, 1/1.5 and 1/2 hydrocortisone/HP-β-CyD molar ratios, separately, which corresponded to hydrocortisone contents of 32%, 20%, 14% and 11% (w/w, with respect to the total sample amount) for the ultimate electrospun nanofibers of hydrocortisone/HP-β-CyD, respectively. The hydrocortisone/HP-β-CyD aqueous systems were stirred for 24 hours at room temperature in order to obtain inclusion complexes. The hydrocortisone/HP-β-CyD (1/0.5, 1/1 and 1/1.5) solutions were turbid due to undissolved hydrocortisone whereas the hydrocortisone/HP-β-CyD (1/2) solution was clear by the end of 24 hours mixing. The pristine HP-β-CyD nanofibers were produced for comparative studies and the uniform nanofiber morphology was ensured by electrospinning of 200% HP-β-CyD (w/v) concentration in aqueous solution.

The electrospinning equipment (Okyay Tech, model: SG10, Turkey) was used for the nanofiber production. The solution of HP-β-CyD and hydrocortisone/HP-β-CyD (1/0.5, 1/1, 1/1.5 and 1/2, molar ratio) was loaded into a 1 mL syringe fixed with a 27 G metal needle, separately. Then, the loaded syringe was positioned onto the syringe pump and the flow rate was set to 0.5 mL h^{-1}. A high voltage power supply ensured a stable voltage of 15 kV during the electrospinning process, and the nanofibers were deposited on a grounded metal collector that was covered with a piece of aluminium foil sheet and located at a distance of 15 cm from the tip of the needle. The electrospinning was performed under ambient conditions where the temperature and humidity were set at 20 °C and 55%, respectively. The electrospun nanofibers obtained from pristine HP-β-CyD solution and hydrocortisone/HP-β-CyD (1/1, 1/1.5 and 1/2, molar ratio) solutions are denoted as HP-β-CyD nanofibers, hydrocortisone/HP-β-CyD (1/1) nanofibers, hydrocortisone/HP-β-CyD (1/1.5) nanofibers and hydrocortisone/HP-β-CyD (1/2) nanofibers. For comparison, a physical mixture of the hydrocortisone/HP-β-CyD (1/1) system was prepared, as well. The pristine HP-β-CyD nanofibrous web (~25 mg) was homogeneously blended with hydrocortisone powder (~6.5 mg) to obtain the hydrocortisone/HP-β-CyD (1/1) physical mixture.

Characterization

Morphological analysis. The morphological examination of nanofibers of HP-β-CyD and hydrocortisone/HP-β-CyD (1/1, 1/1.5 and 1/2) was carried out using a scanning electron microscope (SEM, Tescan MIRA3, Czech Republic). Prior to the measurements, nanofibrous webs were fixed onto SEM stubs using carbon tape and sputtered with a thin layer of Au/Pd to avoid charging during SEM imaging. The working distance and accelerating voltage were set as 10 mm and 12 kV, respectively, for the SEM imaging. The average fiber diameter (AFD) of nanofibers was calculated using ImageJ software (~100 fibers) from different locations of SEM images.

The two main parameters influencing the morphology of nanofibers, viscosity and conductivity of the solutions, were also determined as a part of this study. The viscosity of the HP-β-CyD solution and hydrocortisone/HP-β-CyD solutions (1/1, 1/1.5 and 1/2, molar ratio) was determined using a rheometer (AR 2000 rheometer, TA Instrument, USA) fitted with a 20 mm cone/plate accessory (CP 20–4 spindle type, 4°) under the shear rate range of 0.01–1000 s^{-1} at 22 °C. The conductivity of the same solutions was measured using a conductivity-meter (FiveEasy, Mettler Toledo, USA) at room temperature.

FTIR analysis. The Fourier transform infrared (FTIR) spectra of the hydrocortisone powder, HP-β-CyD nanofibers, hydrocortisone/HP-β-CyD (1/1, 1/1.5 and 1/2) nanofibers and hydrocortisone/HP-β-CyD (1/1) physical mixture were obtained using an attenuated total reflectance Fourier transform infrared (ATR-FTIR) spectrometer (PerkinElmer, USA). The spectra were recorded between 4000 and 600 cm^{-1} at a resolution of 4 cm^{-1} and upon 64 scans.

Thermal analysis. The thermal characteristics of the samples were investigated using a thermogravimetric analyzer (TGA, Q500, TA Instruments, USA) and differential scanning calorimeter (DSC, Q2000, TA Instruments, USA). TGA measurements were performed under a N_2 atmosphere and the samples put onto a platinum TGA pan were heated from room temperature to 550 °C at a heating rate of 20 °C min^{-1}. Prior to the DSC measurements, the samples were sealed in a Tzero aluminum pan. Then, the samples were heated at a flow rate of 10 °C min^{-1} from 0 °C to 240 °C under a N_2 atmosphere.

XRD analysis. An X-ray diffractometer (Bruker D8 Advance ECO) was used to investigate the X-ray diffraction (XRD)

patterns of the hydrocortisone powder, HP-β-CyD nanofibers, hydrocortisone/HP-β-CyD (1/1, 1/1.5 and 1/2) nanofibers and hydrocortisone/HP-β-CyD (1/1) physical mixture. The XRD graphs were recorded between 2θ angles of 5° and 30° by applying Cu-Kα radiation. The voltage and current were set to 40 kV and 25 mA, respectively.

^{1}H-NMR analysis. Proton nuclear magnetic resonance (^{1}H-NMR) spectra were recorded using a nuclear magnetic resonance spectrometer (Bruker AV500, with an autosampler) at 25 °C. The molar ratio between hydrocortisone and HP-β-CyD in hydrocortisone/HP-β-CyD nanofibers was calculated by ^{1}H-NMR. For ^{1}H-NMR measurements, hydrocortisone powder, HP-β-CyD nanofibers, and hydrocortisone/HP-β-CyD (1/1, 1/1.5 and 1/2) nanofibers were dissolved in *d6*-DMSO at a 40 g L^{-1} sample concentration. The ^{1}H-NMR spectra were scanned 16 times and Mestrenova software was used to achieve the integration of chemical shifts (δ, ppm) for each sample. Then, the peaks of hydrocortisone (–CH_3; 0.75 ppm) and HP-β-CyD (–CH_3; 1.03 ppm) were used to calculate the molar ratio of hydrocortisone/HP-β-CyD in hydrocortisone/HP-β-CyD (1/1, 1/1.5 and 1/2) nanofibers.

Phase solubility profile of the hydrocortisone/HP-β-CyD system. Phase solubility analysis of hydrocortisone was performed according to a method reported by Higuchi and Connors.[57] A definite amount of hydrocortisone above its solubility and HP-β-CyD powder with an increasing concentration (0–8 mM) were put into glass vials, separately, and then 5 mL of water was added to each vial. The vials were sealed, shielded from light and shaken for 24 hours on an incubator shaker at 25 °C and 450 rpm. Afterwards, the suspensions were filtered with a 0.45 μm PTFE filter. The filtered aliquots were measured using UV-vis-spectroscopy (PerkinElmer, Lambda 35) to calculate the amount of hydrocortisone dissolved. The experiments were performed in triplicate (n = 3) and the average absorption results were adapted to concentration (mM) using a calibration curve which showed linearity and acceptability with $R^2 \geq 0.99$. Then, the phase solubility diagram was plotted in order to calculate the binding constant (Ks) from the following equation:

$$\text{Ks} = \text{slope}/S_0(1 - \text{slope}) \quad (1)$$

where S_0 is the intrinsic solubility of hydrocortisone in the absence of HP-β-CyD.

***In vitro* release test.** The time dependent release profiles of hydrocortisone/HP-β-CyD (1/1, 1/1.5 and 1/2) nanofibrous webs at the same weight of ~40 mg was investigated in distilled water (50 mL) at room temperature. For comparison, ~8 mg of hydrocortisone powder was also examined which corresponded to the theoretical hydrocortisone content in hydrocortisone/HP-β-CyD (1/1) nanofibers. For the test, the nanofibrous webs and hydrocortisone powder were precisely weighed and placed into a beaker and then the water medium was poured into the samples. The solutions were shaken with a speed of 200 rpm and 0.5 mL of sample solution was withdrawn and an equal amount of fresh medium was refilled at the given time points. The dissolved amount of hydrocortisone was analyzed using UV-vis-spectroscopy at a wavelength of 248 nm. The calibration curve of hydrocortisone showed linearity and acceptability with $R^2 \geq 0.99$, and measurement results were adapted to this calibration curve to convert absorbance to concentration (μg mL^{-1}). The experiments were performed three times and the results were reported as average.

Solubility, dissolution and disintegration profile of hydrocortisone/HP-β-CyD nanofibrous webs. The solubility enhancement of hydrocortisone encapsulated in hydrocortisone/HP-β-CyD nanofibers was also indicated after long term stirring of the hydrocortisone powder and hydrocortisone/HP-β-CyD nanofiber solutions (24 hours). For this experiment, ~2.2 mM hydrocortisone powder and hydrocortisone/HP-β-CyD (1/1) nanofibers (~20 mg), hydrocortisone/HP-β-CyD (1/1.5) nanofibers (~28 mg) and hydrocortisone/HP-β-CyD (1/2) nanofibers (~35 mg) that have the same amount of hydrocortisone were stirred in distilled water (5 mL) for 24 hours at 150 rpm. Then, the solutions were filtered using a 0.45 μm PTFE filter and their UV-vis absorbance was measured in the range of 190–340 nm.

For the dissolution test, ~6 mg of hydrocortisone/HP-β-CyD nanofibrous webs (1/1, 1/1.5 and 1/2) (~2 cm × 1.2 cm) and ~1.2 mg of hydrocortisone powder were immersed in 4 mL of distilled water in plastic Petri dishes. Here, the amount of hydrocortisone powder (~1.2 mg) was determined according to the hydrocortisone content of ~6 mg hydrocortisone/HP-β-CyD (1/1) nanofibrous web which has the highest drug content of 20% (w/w). During the immersion, a video was recorded concurrently in order to follow the dissolution.

Bi *et al.* reported a technique in which the physiological conditions under the surface of a moist tongue were simulated.[58] Here, the disintegration profiles of hydrocortisone/HP-β-CyD nanofibrous webs were investigated with a slightly modified version of this method. Firstly, pieces of filter paper having a suitable size were placed in plastic Petri dishes (10 cm), and then they were wetted with 10 mL of artificial saliva (2.38 g Na_2HPO_4, 0.19 g KH_2PO_4 and 8 g NaCl were dissolved in 1 L distilled water, pH was adjusted to 6.8 by addition of phosphoric acid). Afterwards, the excess artificial saliva was completely removed from the Petri dishes and a piece of hydrocortisone/HP-β-CyD (1/1, 1/1.5 and 1/2) nanofibrous web (~3 cm × 3.7 cm) was placed at the centre of the filter paper. The disintegration of hydrocortisone/HP-β-CyD (1/1, 1/1.5 and 1/2) nanofibrous webs was recorded as a video.

Results and discussion

Electrospinning of nanofibers

Typically, organic solvents or organic solvent/water mixtures are used to dissolve both polymeric matrices and hydrophobic drugs for the electrospinning of drug/polymer based fast-dissolving nanofibers.[21,59] Even though most of the organic solvents evaporate during electrospinning, the use of organic solvents for the electrospinning process and the possibility of

remaining toxic organic solvent residues in the fiber matrix may be quite problematic for these drug formulations in the pharmaceutical industry. On the other hand, the use of CyDs as a fiber matrix offers a great advantage since hydrophobic drug molecules become water-soluble by inclusion complexation with CyDs, therefore, the electrospinning of drug/CyD systems can be performed in water in order to produce fast-dissolving nanofibers.[8,14] Here, the electrospinning solution of hydrocortisone/HP-β-CyD complex was prepared in water by using a high concentration of HP-β-CyD (180%, w/v) (Fig. 1). Initially, aqueous solutions of hydrocortisone/HP-β-CyD having 1/0.5, 1/1, 1/1.5 and 1/2 molar ratios were prepared for the electrospinning (Fig. 1d). The hydrocortisone/HP-β-CyD (1/0.5, 1/1 and 1/1.5) systems were turbid due to the presence of uncomplexed/undissolved hydrocortisone. The hydrocortisone/HP-β-CyD (1/0.5) solution was very heterogeneous and very turbid due to the presence of a high amount of undissolved hydrocortisone since a low amount of HP-β-CyD was used. Yet, the turbidity was lower for hydrocortisone/HP-β-CyD (1/1) and it was much lower for hydrocortisone/HP-β-CyD (1/1.5) since a higher amount of hydrocortisone became soluble as the amount of HP-β-CyD was increased. In contrast, the hydrocortisone/HP-β-CyD aqueous solution having a 1/2 molar ratio resulted in a clear solution since the hydrocortisone become fully water-soluble by HP-β-CyD inclusion complexation (Fig. 1d). The electrospinning was performed in order to produce nanofibers from hydrocortisone/HP-β-CyD (1/0.5, 1/1, 1/1.5 and 1/2) systems. Since the hydrocortisone/HP-β-CyD (1/0.5) solution was very heterogeneous due to the presence of a high amount of undissolved hydrocortisone, the electrospinning of the hydrocortisone/HP-β-CyD (1/0.5) aqueous system was unsuccessful in which we could not obtain nanofibers. On the other hand, the electrospinning of hydrocortisone/HP-β-CyD aqueous solutions having 1/1, 1/1.5 and 1/2 molar ratios was successful resulting in uniform and bead-free electrospun nanofibers (Fig. 2b–d). As a control sample, pristine HP-β-CyD nanofibers without hydrocortisone was also electrospun in which 200% (w/v) HP-β-CyD aqueous solution was used to produce bead-free nanofibers (Fig. 2a). Even though the hydrocortisone/HP-β-CyD (1/1 and 1/1.5) solutions contained undissolved hydrocortisone crystals, the SEM images of electrospun hydrocortisone/HP-β-CyD (1/1 and 1/1.5) nanofibers did not show any hydrocortisone crystals suggesting that the hydrocortisone crystals are small in size and homogeneously distributed within the fiber matrix (Fig. 2b and c). The fiber

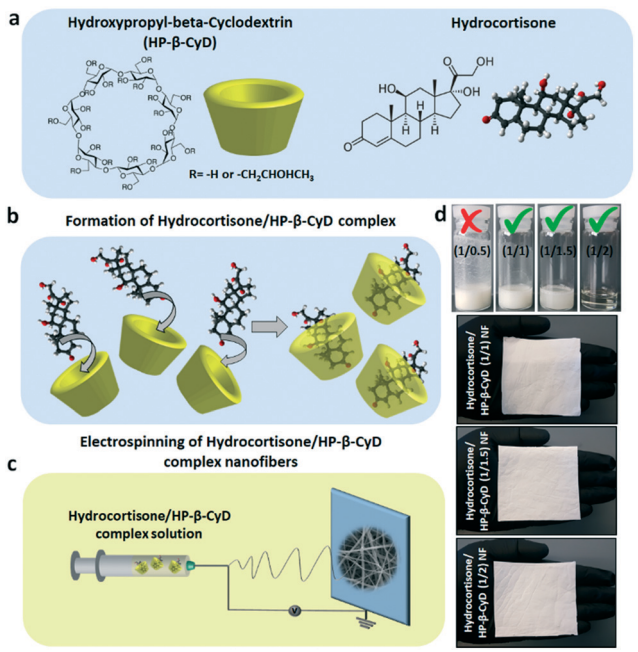

Fig. 1 (a) Chemical structure and schematic illustration of HP-β-CyD and hydrocortisone molecules. Schematic representation of the (b) formation of the hydrocortisone/HP-β-CyD complex and (c) electrospinning of hydrocortisone/HP-β-CyD complex nanofibers and (d) the photographs of hydrocortisone/HP-β-CyD (1/1, 1/1.5 and 1/2) solutions and the resulting electrospun nanofibrous webs.

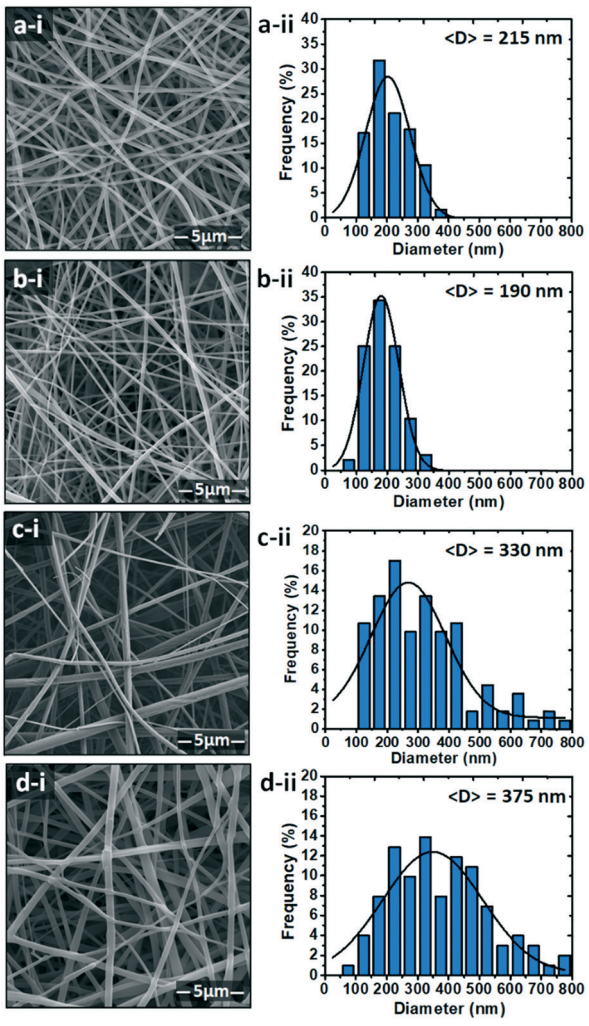

Fig. 2 SEM images and the fiber diameter distribution graphs of (a-i and ii) HP-β-CyD nanofibers, (b-i and ii) hydrocortisone/HP-β-CyD (1/1) nanofibers, (c-i and ii) hydrocortisone/HP-β-CyD (1/1.5) nanofibers and (d-i and ii) hydrocortisone/HP-β-CyD (1/2) nanofibers.

diameter distribution was between 90 and 320 nm having an average fiber diameter of 190 ± 55 nm for hydrocortisone/HP-β-CyD (1/1) nanofibers. For hydrocortisone/HP-β-CyD (1/1.5) nanofibers, the fiber diameter distribution was between 110 and 770 nm having an average fiber diameter of 330 ± 165 nm. The hydrocortisone/HP-β-CyD (1/2) nanofibers have a fiber diameter distribution between 70 and 790 nm with an average fiber diameter of 375 ± 160 nm (Table 1). The different fiber diameter values for the hydrocortisone/HP-β-CyD (1/1, 1/1.5 and 1/2) nanofibers were due to the different viscosity and conductivity values of the hydrocortisone/HP-β-CyD solutions. Even though the hydrocortisone/HP-β-CyD (1/1) solution had a higher viscosity value than the hydrocortisone/HP-β-CyD (1/1.5 and 1/2) solutions, the conductivity of the hydrocortisone/HP-β-CyD (1/1) solution was also higher which resulted in thinner fibers during electrospinning. The pristine HP-β-CyD solution had the highest viscosity value compared to the hydrocortisone/HP-β-CyD solutions since a higher concentration (200%, w/v) was used for the electrospinning of pure HP-β-CyD nanofibers. In addition, the conductivity of the HP-β-CyD solution was very close to that of the hydrocortisone/HP-β-CyD (1/1) solution but it was higher than those of the hydrocortisone/HP-β-CyD (1/1.5 and 1/2) solutions. Therefore, the electrospinning of pristine HP-β-CyD nanofibers resulted in an average fiber diameter of 215 ± 65 nm where the fiber diameter distribution was between 100 and 360 nm. The hydrocortisone/HP-β-CyD (1/1.5) solution had a higher viscosity and a higher conductivity value than the hydrocortisone/HP-β-CyD (1/2) solution, so, the average fiber diameter of the hydrocortisone/HP-β-CyD (1/1.5) nanofibers was slightly less than that of the hydrocortisone/HP-β-CyD (1/2) nanofibers due to their higher solution conductivity. In general, solutions having higher conductivity yield thinner fibers upon more stretching of the jet during electrospinning.[60,61] Hence, the trend in different fiber diameters among HP-β-CyD nanofibers and hydrocortisone/HP-β-CyD (1/1, 1/1.5 and 1/2) nanofibers correlates with the literature. Moreover, the electrospinning of hydrocortisone/HP-β-CyD (1/1, 1/1.5 and 1/2) solutions resulted in uniform nanofibers in the form of nanofibrous webs having a self-standing characteristic (Fig. 1d) that would be quite suitable for fast-dissolving oral drug delivery systems.

Structural characterization

FTIR is a suitable technique to prove the existence of guest molecules in the inclusion complex nanofibers.[8,33] FTIR is also a convenient approach to examine the formation of inclusion complexes between CyD and guest molecules owing to broadening, shifts, disappearance and/or attenuation in the characteristic peaks of guest molecules due to interaction with CyD cavities.[62,63] The FTIR spectra of the hydrocortisone powder, HP-β-CyD nanofibers, hydrocortisone/HP-β-CyD (1/1, 1/1.5 and 1/2) nanofibers and hydrocortisone/HP-β-CyD (1/1) physical mixture are shown in Fig. 3. In the full range FTIR spectra of the samples, there exists a noticeable stretching peak between 3000 and 3600 cm^{-1} which corresponds to the –OH groups of HP-β-CyD.[8,33] The other prominent absorption bands are observed at around the 1020 and 1150 cm^{-1} region due to the vibrations of coupled C–C/C–O stretching and antisymmetric C–O–C glycosidic bridge stretching.[8,33] It is challenging to obtain evidence about the inclusion complexation from this region, since the higher amount of CyD in the inclusion complex formulation causes overlapping and so, characteristic peaks of guest molecules are masked inherently. Nevertheless, a strong band of hydrocortisone appearing at the range of 1642–1709 cm^{-1} corresponding to the C═O bending was observed in the FTIR spectra of hydrocortisone/HP-β-CyD (1/1, 1/1.5 and 1/2) nanofibers (Fig. 3b).[64] These findings proved the presence of hydrocortisone in the samples of hydrocortisone/HP-β-CyD (1/1, 1/1.5 and 1/2) nanofibers. Furthermore, the C═O bending peak of hydrocortisone is reduced in intensity and shifted from the range of 1642–1709 cm^{-1} to 1653–1714 cm^{-1} in the case of hydrocortisone/HP-β-CyD (1/1, 1/1.5 and 1/2) nanofibers due to the complexation (Fig. 3b). On the other hand, there is no shift for the same peaks of hydrocortisone in the hydrocortisone/HP-β-CyD (1/1) physical mixture.[64] Moreover, the other characteristic peaks of hydrocortisone became obvious in the case of the hydrocortisone/HP-β-CyD (1/1) physical mixture (Fig. 3c) because of the uncomplexed state of hydrocortisone. Briefly, the FTIR analysis validates the presence of hydrocortisone in hydrocortisone/HP-β-CyD nanofibers and asserts that the hydrocortisone is encapsulated in the HP-β-CyD by inclusion complexation.

Typically, poorly water-soluble drug molecules and polymeric carrier matrices are both dissolved in common solvent systems or in mixed solvent systems in order to prepare electrospinning solutions. The electrospinning technique has the advantage because the solvent rapidly evaporates during the electrospinning process as the electrified fluid jet solidifies in the form of fibers. The rapid solidification of the polymeric fiber matrix reduces the mobility of the drug molecules so that the drug molecules cannot come into contact with

Table 1 The solution properties and the fiber diameters of the resulting electrospun nanofibers

Sample	HP-β-CyD concentration (%, w/v)	Molar ratio of hydrocortisone/HP-β-CyD	Viscosity (Pa S)	Conductivity (μS cm^{-1})	Average fiber diameter (nm)
HP-β-CyD	200	—	1.533	36.3	215 ± 65
Hydrocortisone/HP-β-CyD (1/1)	180	1/1	1.395	37.6	190 ± 55
Hydrocortisone/HP-β-CyD (1/1.5)	180	1/1.5	1.339	34.7	330 ± 165
Hydrocortisone/HP-β-CyD (1/2)	180	1/2	1.156	28.9	375 ± 160

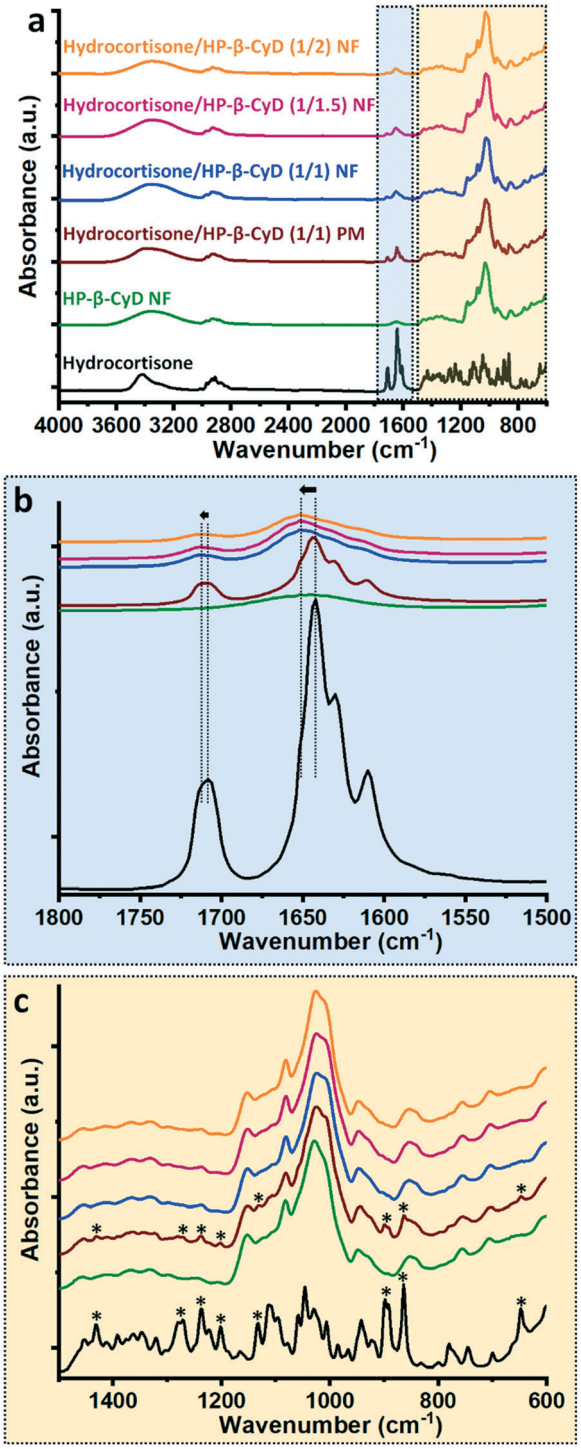

Fig. 3 (a) The full and (b and c) expanded range FTIR spectra of the hydrocortisone powder, HP-β-CyD nanofibers (NF), hydrocortisone/HP-β-CyD (1/1, 1/5 and 1/2) nanofibers (NF) and hydrocortisone/HP-β-CyD (1/1) physical mixture (PM).

each other to form crystals. Therefore, drug molecules are often present in the amorphous physical state and distributed homogeneously within the electrospun nanofiber matrix.[21,59] The amorphous nature of the drug molecules encapsulated in fiber matrices along with the very large surface area and highly porous characteristics of electrospun nanofibrous webs facilitates their fast-dissolution.[21] XRD is a useful technique to investigate whether the drug molecules are in the crystalline form or in the amorphous state in the electrospun nanofiber matrix.[10,59,65]

XRD is also a very handy analytical technique to characterize the inclusion complexation of CyDs with guest molecules.[62,63] In the case of inclusion complexation, the guest molecules reside in the CyD cavity and separate from each other, and therefore cannot form crystals.[63] The XRD patterns of pure hydrocortisone, hydrocortisone/HP-β-CyD (1/1, 1/1.5 and 1/2) nanofibers and the physical mixture of hydrocortisone/HP-β-CyD (1/1) are shown in Fig. 4. Hydrocortisone is a crystalline drug molecule which has distinct diffraction peaks at 14.4°, 15.2° and 17.4° (Fig. 4). The hydrocortisone/HP-β-CyD (1/1 and 1/1.5) solutions were turbid indicating the presence of undissolved/uncomplexed hydrocortisone crystals. The XRD data of hydrocortisone/HP-β-CyD nanofibers correlate with the visual observation of their solutions. The XRD pattern of hydrocortisone/HP-β-CyD (1/1) nanofibers has shown the characteristic diffraction peaks of hydrocortisone signifying that some hydrocortisone molecules are present in the crystal form in the nanofiber matrix. The hydrocortisone/HP-β-CyD (1/1) physical mixture was also prepared and analyzed for comparison. The XRD peaks of hydrocortisone in hydrocortisone/HP-β-CyD (1/1) nanofibers were less intense than those in the hydrocortisone/HP-β-CyD (1/1) physical mixture even though these two samples have the same amount of hydrocortisone. This indicates that some hydrocortisone was complexed within HP-β-CyD whereas some uncomplexed hydrocortisone was in the crystalline from in the hydrocortisone/HP-β-CyD (1/1) nanofiber matrix. The XRD pattern of hydrocortisone/HP-β-CyD (1/1.5) nanofibers has shown very low

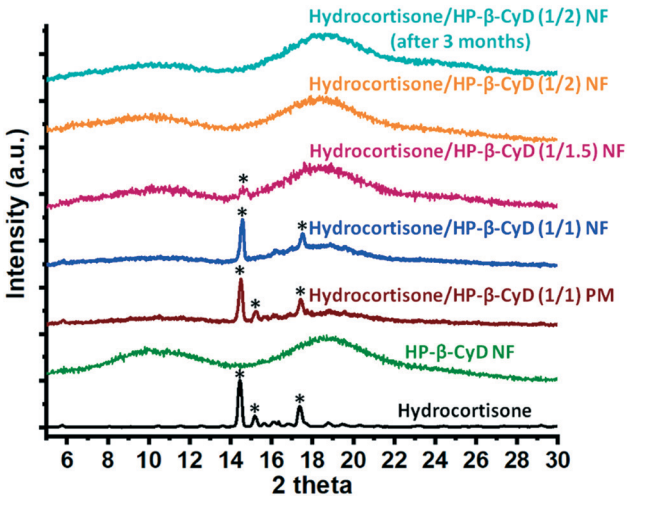

Fig. 4 XRD patterns of the hydrocortisone powder, HP-β-CyD nanofibers (NF), hydrocortisone/HP-β-CyD (1/1, 1/5 and 1/2) nanofibers (NF), hydrocortisone/HP-β-CyD (1/2) nanofibers (NF) after 3 months of storage (at 55–65% RH and ~22 °C) and hydrocortisone/HP-β-CyD (1/1) physical mixture (PM).

intensity for hydrocortisone crystals suggesting that very little amounts of uncomplexed hydrocortisone were present in this sample. The XRD data correlate with the visual observation of the hydrocortisone/HP-β-CyD (1/1.5) solution, which was much less turbid than the hydrocortisone/HP-β-CyD (1/1) solution indicating that a much lower amount of uncomplexed/undissolved hydrocortisone was present in this solution (Fig. 1d). Even though the XRD data have clearly proven the presence of some hydrocortisone crystals in hydrocortisone/HP-β-CyD (1/1 and 1/1.5) nanofibers, the hydrocortisone crystals were not seen in the SEM image of hydrocortisone/HP-β-CyD (1/1 and 1/1.5) nanofibers (Fig. 2b and c), suggesting that the hydrocortisone crystals are not coarse but rather distributed homogeneously in small sizes within the nanofiber matrix. On the other hand, the hydrocortisone/HP-β-CyD (1/2) solution was clear indicating that hydrocortisone molecules are totally complexed with HP-β-CyD and become water soluble (Fig. 1d). As anticipated, no diffraction peaks of hydrocortisone were recorded for the hydrocortisone/HP-β-CyD (1/2) complex nanofibers elucidating that hydrocortisone molecules are inside the HP-β-CyD cavity and the inclusion complexation prevents the crystallization of hydrocortisone molecules. The XRD pattern of hydrocortisone/HP-β-CyD (1/2) complex nanofibers has a broad halo pattern similar to that of pristine HP-β-CyD nanofibers indicating that the amorphization of hydrocortisone is achieved by inclusion complexation. In addition, there was no sign of recrystallization of hydrocortisone even after 3 months of storage at 55–65% RH and at ~22 °C, indicating the stability of the hydrocortisone/HP-β-CyD (1/2) complex nanofibers (Fig. 4). The hydrocortisone/HP-β-CyD (1/2) nanofibrous web still kept its fibrous structure and it was intact keeping its self-standing and flexible character (Fig. S1†). The pristine HP-β-CyD is an amorphous molecule[66] and therefore the electrospun HP-β-CyD nanofibers have a broad halo diffraction pattern. It is important to note that the amorphous state of hydrocortisone is preferred which facilitates its fast-dissolution. The dissolution tests which will be discussed below indicated that the hydrocortisone/HP-β-CyD (1/2) complex nanofibrous matrix has shown a fast-dissolving behaviour due to the complete inclusion complexation of hydrocortisone with HP-β-CyD along with the highly porous structure and high surface area of the nanofibrous webs and the highly water-soluble nature of HP-β-CyD as a nanofiber matrix.

The thermal characteristics of the hydrocortisone/HP-β-CyD nanofibers were investigated by differential scanning calorimetry (DSC). DSC is a useful technique to investigate the presence of crystals by observation of the melting point. In addition, DSC provides useful information on inclusion complexation between CyD and host molecules.[63] For instance, the melting point of guest molecules disappears in the case of inclusion complexation since guest molecules are separated from each other by the CyD cavity and therefore cannot form crystals.[63] The DSC thermogram of pure hydrocortisone reveals its crystalline nature showing a distinct melting peak at 222 °C (Fig. 5). The pristine HP-β-CyD nanofibers are in

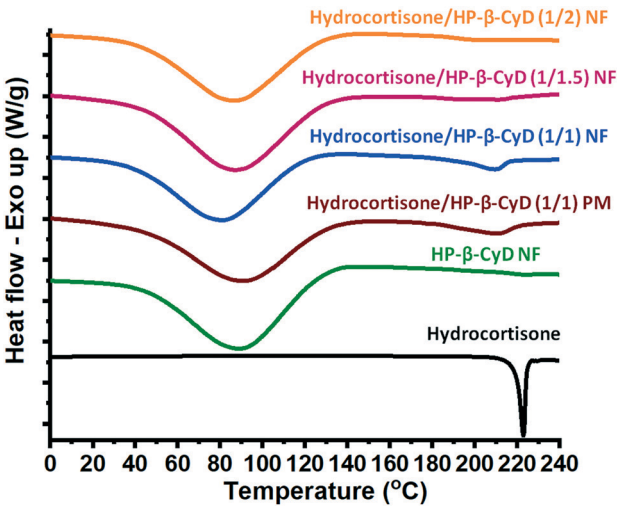

Fig. 5 DSC thermograms of the hydrocortisone powder, HP-β-CyD nanofibers (NF), hydrocortisone/HP-β-CyD (1/1, 1/5 and 1/2) nanofibers (NF), and hydrocortisone/HP-β-CyD (1/1) physical mixture (PM).

the amorphous state and have shown a broad peak in the range of 30–140 °C due to water loss.[67] The DSC thermogram of hydrocortisone/HP-β-CyD (1/1) nanofibers shows an endothermic peak at 209 °C having a peak area of ~13.5 J g^{-1} due to the melting of hydrocortisone crystals. The physical mixture of hydrocortisone/HP-β-CyD (1/1) has also shown a melting peak at 210 °C with a peak area of 18.5 J g^{-1}. The recorded melting peak area for hydrocortisone/HP-β-CyD (1/1) nanofibers was less than the melting peak area for the physical mixture of hydrocortisone/HP-β-CyD (1/1). This suggests that hydrocortisone was partially complexed with HP-β-CyD but the major amount of hydrocortisone was in the uncomplexed state in hydrocortisone/HP-β-CyD (1/1) nanofibers. The DSC thermogram of hydrocortisone/HP-β-CyD (1/1.5) nanofibers shows the melting of hydrocortisone crystals at 210 °C having a peak area of ~1.1 J g^{-1}. Yet, the melting peak area for hydrocortisone/HP-β-CyD (1/1.5) nanofibers was much smaller than the melting peak area of hydrocortisone/HP-β-CyD (1/1) nanofibers, which clearly confirmed that the amount of crystalline hydrocortisone in the hydrocortisone/HP-β-CyD (1/1.5) nanofibers is much lower than that in the hydrocortisone/HP-β-CyD (1/1) nanofibers. In the case of hydrocortisone/HP-β-CyD (1/2) nanofibers, there was no melting peak recorded for hydrocortisone suggesting that hydrocortisone was fully in the inclusion complexation state in the nanofiber matrix. The hydrocortisone/HP-β-CyD (1/2) solution was clear and homogeneous (Fig. 1d) indicating that hydrocortisone was fully dissolved by HP-β-CyD inclusion complexation. In short, the DSC data correlate with the XRD data and visual observations of the hydrocortisone/HP-β-CyD solutions (1/1, 1/1.5 and 1/2). Hydrocortisone was fully in the amorphous state in hydrocortisone/HP-β-CyD (1/2) nanofibers whereas it was mostly crystalline in hydrocortisone/HP-β-CyD (1/1) nanofibers and there were very little amounts of crystalline hydrocortisone in hydrocortisone/HP-β-CyD (1/1.5) nanofibers.

TGA measurements of the hydrocortisone powder, HP-β-CyD nanofibers and hydrocortisone/HP-β-CyD (1/1, 1/1.5 and 1/2) nanofibers were performed by thermo-analytical studies (Fig. 6). The hydrocortisone powder exhibits a mass loss that starts at 205 °C and ends at 500 °C. In the case of pristine HP-β-CyD nanofibers, there are two main weight losses from 25 °C and 400 °C which correspond to water loss (up to 100 °C) and the main degradation of HP-β-CyD (max. temp 358 °C). As it is shown in Fig. 6, the main degradation of hydrocortisone occurs at the similar temperature range of HP-β-CyD degradation, therefore two steps of mass losses are also observed for hydrocortisone/HP-β-CyD (1/1, 1/1.5 and 1/2) nanofibers. On the other hand, the derivative curve of HP-β-CyD nanofibers became wider and reduced in intensity in the case of hydrocortisone/HP-β-CyD (1/1, 1/1.5 and 1/2) nanofibers due to the hydrocortisone content in these samples (Fig. 6b). While the main degradation of HP-β-CyD starts at 280 °C for HP-β-CyD nanofibers, it shifts to lower temperatures of 233 °C, 238 °C and 244 °C for hydrocortisone/HP-β-CyD (1/1) nanofibers, hydrocortisone/HP-β-CyD (1/1.5) nanofibers and hydrocortisone/HP-β-CyD (1/2) nanofibers, respectively. Even the third step mass loss of the hydrocortisone powder becomes apparent for hydrocortisone/HP-β-CyD (1/1) nanofibers at 430 °C due to their higher hydrocortisone content compared to hydrocortisone/HP-β-CyD (1/2) nanofibers.

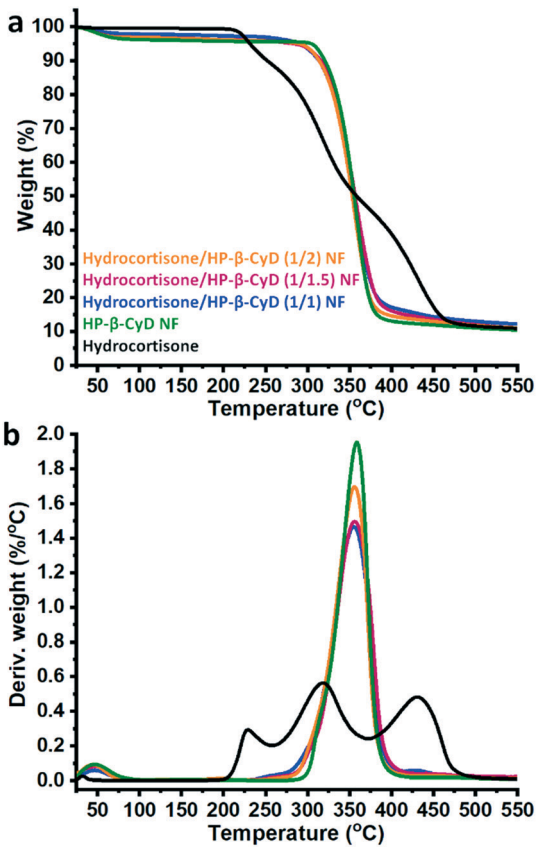

Fig. 6 (a) TGA thermograms and (b) derivatives of hydrocortisone powder, HP-β-CyD nanofibers (NF) and hydrocortisone/HP-β-CyD (1/1, 1/1.5 and 1/2) nanofibers (NF).

Since hydrocortisone/HP-β-CyD (1/1) nanofibers contain a higher amount of hydrocortisone (20% (w/w), with respect to the total sample amount) than hydrocortisone/HP-β-CyD (1/1.5) nanofibers (14% (w/w), with respect to the total sample amount) and hydrocortisone/HP-β-CyD (1/2) nanofibers (11% (w/w), with respect to the total sample amount), the main degradation profile of HP-β-CyD probably shifts to a lower temperature in the case of hydrocortisone/HP-β-CyD (1/1) nanofibers (233 °C) compared to hydrocortisone/HP-β-CyD (1/2) complex nanofibers (238 °C) and hydrocortisone/HP-β-CyD (1/2) complex nanofibers (244 °C) (Fig. 6b). Actually, it is also possible to calculate the component ratios in the samples by the TGA technique. However, the degradation step of hydrocortisone is overlapped with the main degradation of HP-β-CyD in the case of hydrocortisone/HP-β-CyD (1/1, 1/1.5 and 1/2) nanofibers (Fig. 6b) which makes it difficult to calculate the content of hydrocortisone in hydrocortisone/HP-β-CyD (1/1, 1/1.5 and 1/2) nanofibers from the TGA data. Essentially, the increase in thermal stability of guest molecules is very common for the CyD complex and considered as evidence of inclusion complexation.[63] Here, TGA revealed the interaction between hydrocortisone and HP-β-CyD in hydrocortisone/HP-β-CyD (1/1, 1/1.5 and 1/2) nanofibers by means of altered degradation profiles of HP-β-CyD molecules.

^{1}H-NMR analysis was carried out to determine the molar ratio between hydrocortisone and HP-β-CyD in electrospun hydrocortisone/HP-β-CyD nanofibers. The initial molar ratio between hydrocortisone and HP-β-CyD in hydrocortisone/HP-β-CyD solutions were determined to be 1/1, 1/1.5 and 1/2 prior to the electrospinning. However, the molar ratio may change for hydrocortisone/HP-β-CyD nanofibers depending on the encapsulation efficiency of the electrospinning process. Here, the molar ratio of each hydrocortisone/HP-β-CyD system was calculated by using the proportion of the integrated peaks of hydrocortisone and HP-β-CyD. For hydrocortisone/HP-β-CyD (1/1, 1/1.5 and 1/2) nanofibers, the $-CH_3$ protons of hydrocortisone (0.75 ppm) and HP-β-CyD (1.03 ppm) were used for the calculations (Fig. 7).[47]

As observed in Fig. 7, the given peaks of hydrocortisone and HP-β-CyD are quite suitable for the calculations due to their distinct profiles. It is important to have similar loading of active compounds after electrospinning in order to attain the high yield of drug encapsulation for inclusion complex nanofibers. The ^{1}H-NMR data showed that the molar ratios of hydrocortisone/HP-β-CyD in hydrocortisone/HP-β-CyD (1/1, 1/1.5 and 1/2) nanofibers were the same as the initial ratios of 1/1, 1/1.5 and 1/2. The ^{1}H-NMR findings revealed that the ultimate electrospun hydrocortisone/HP-β-CyD nanofibers were obtained without any loss of hydrocortisone ensuring the initial molar ratios of 1/1, 1.5 and 1/2 (hydrocortisone/HP-β-CyD). As discussed in the DSC and XRD analyses, there is uncomplexed hydrocortisone in the case of hydrocortisone/HP-β-CyD (1/1 and 1/1.5) nanofibers. Since the NMR solvent *d6*-DMSO could dissolve the uncomplexed hydrocortisone fraction in the hydrocortisone/HP-β-CyD (1/1 and 1/1.5) nanofibers, the exact and the initial molar ratios of 1/1 and 1/1.5

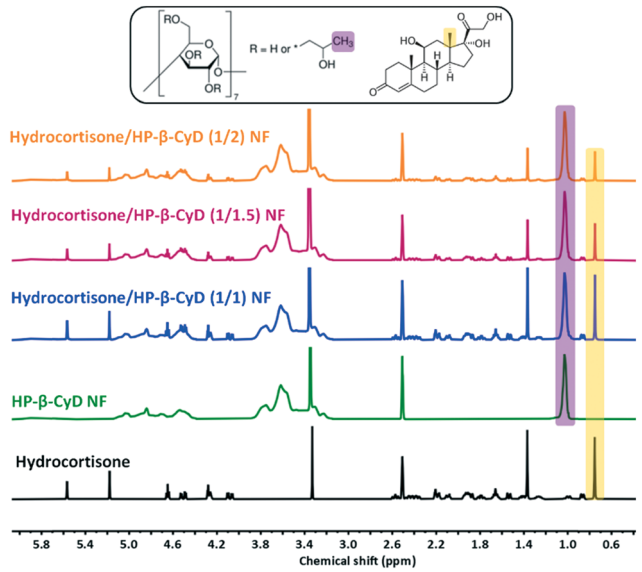

Fig. 7 ^{1}H-NMR spectra of pure hydrocortisone, HP-β-CyD nanofibers (NF), and hydrocortisone/HP-β-CyD (1/1, 1/1.5 and 1/2) nanofibers (NF). ^{1}H-NMR spectra were recorded by dissolving the samples in *d6*-DMSO. The characteristic peaks of hydrocortisone and HP-β-CyD are highlighted with yellow and purple colors, respectively.

were calculated from the ^{1}H-NMR spectra. The results confirmed that electrospinning is an efficient encapsulation technique where hydrocortisone/HP-β-CyD nanofibers can be successfully produced along with a desired hydrocortisone content and without any loss.

Solubility, dissolution and disintegration profile of hydrocortisone/HP-β-CyD nanofibrous webs

Phase solubility tests are commonly performed to obtain information about the solubilizing effect of CyD on hydrophobic drug molecules. Additionally, phase solubility diagrams enable calculations of the stability constants of inclusion complexes formed between CyD and drug molecules.[46,68,69] In this study, the dynamic equilibrium of hydrocortisone/HP-β-CyD solutions having different HP-β-CyD concentrations reached up to 24 hours and the filtered aliquots of the solutions were examined by the UV-vis spectroscopy technique. The phase solubility diagram (Fig. 8a) shows the solubility manner of hydrocortisone against increasing HP-β-CyD concentrations from 0 to 8 mM. The solubility of hydrocortisone was increased ~2.8 times in the 8 mM concentrated solution of HP-β-CyD owing to the inclusion complex formation. According to the method reported by Higuchi and Connors, there are different types of phase solubility diagrams depending on the CyD and guest molecules.[57] The A-type phase solubility diagram is generally observed for modified CyD systems and has subtypes of A_L, A_N and A_P which stand for linear increases in guest solubility as a function of CyD concentration, positive deviation of isotherms and negative deviation of isotherms, respectively.[57,68] In our case, the phase solubility diagram adopts a manner of forming an A_N-

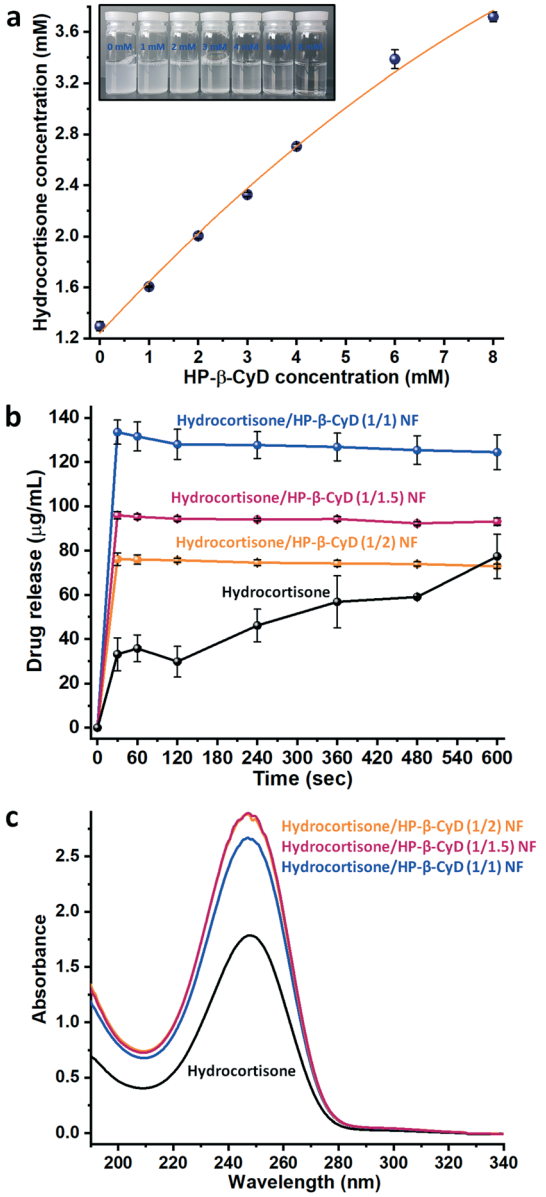

Fig. 8 (a) Phase solubility diagram of the hydrocortisone/HP-β-CyD complex system and the inset photograph of the hydrocortisone/HP-β-CyD systems for different HP-β-CyD concentrations. (b) Time dependent release profiles and (c) UV-vis spectra of aqueous solutions of hydrocortisone and hydrocortisone/HP-β-CyD (1/1, 1/1.5 and 1/2) nanofibers (NF).

type pattern suggesting that the highest HP-β-CyD concentration of 8 mM might be considered as the approximate limits and less effective for the solubilization of hydrocortisone. Using the straight-line portion of the phase solubility diagram, the apparent stability constant (Ks) was calculated according to eqn (1). The Ks value, which essentially represents the binding strength between the CyD cavity and guest molecules, was calculated to be 417 M^{-1} for our hydrocortisone/HP-β-CyD system. Other related studies, in which the inclusion complexes of hydrocortisone and HP-β-CyD were investigated, presented different stability constant values of 636

M^{-1},[70] 1400 M^{-1},[71] 1450 M^{-1} (ref. 72) and 1700 M^{-1} (ref. 73) for the hydrocortisone/HP-β-CyD system. Loftsson *et al.* reported that the variation between the stability constant values for the same drug/CyD system might originate from the degree of substitution (DS) differences of HP groups in HP-β-CyD, and the binding strength between the drug and HP-β-CyD decreases upon increasing the DS.[74] Our data and the previously reported results are in agreement with this proposal.

The stability constant for the hydrocortisone/HP-β-CyD system was reported in the range of 1400–1700 M^{-1} when HP-β-CyD having a DS of ~0.6 was used,[71–73] and a stability constant of 636 M^{-1} was reported for HP-β-CyD having a DS of ~1.[70] In our case, we have obtained a stability constant of 417 M^{-1} for the hydrocortisone/HP-β-CyD system in which the HP-β-CyD we used has a DS of ~0.9.

The comparison of the *in vitro* release profile of hydrocortisone from hydrocortisone/HP-β-CyD (1/1, 1/1.5 and 1/2) nanofibers and hydrocortisone powder is shown in Fig. 8b. The hydrocortisone/HP-β-CyD (1/1, 1/1.5 and 1/2) nanofibrous webs disappeared instantly after they came into contact with the dissolution media. Hydrocortisone/HP-β-CyD (1/1), hydrocortisone/HP-β-CyD (1/1.5) and hydrocortisone/HP-β-CyD (1/2) nanofibrous webs released 133.5 ± 4.7 μg mL^{-1}, 95.9 ± 1.7 μg mL^{-1} and 76.2 ± 2.8 μg mL^{-1} hydrocortisone in the first 30 seconds, respectively confirming their fast-dissolution behavior and all the samples showed a plateau profile up to 10 minutes. On the other hand, the hydrocortisone powder did not dissolve immediately and only 33.1 ± 7.4 μg mL^{-1} hydrocortisone was released into the dissolution medium in the first 30 seconds and it reached up to a concentration of 77.4 ± 10.0 μg mL^{-1} by the end of 10 minutes. This finding verified the significant improvement of the fast-dissolution profile of hydrocortisone in the hydrocortisone/HP-β-CyD nanofibrous webs compared to that of the pure hydrocortisone powder. The enhanced rapid release profile of hydrocortisone from hydrocortisone/HP-β-CyD (1/1, 1/1.5 and 1/2) nanofibrous webs can be attributed to these unique features: (i) inclusion complex formation between hydrocortisone and HP-β-CyD; (ii) the high water-solubility of HP-β-CyD; (iii) the high surface area and highly porous structure of nanofibrous webs which provide an effective penetration path and a higher amount of contact sites for the dissolution media. As seen in Fig. 8b, hydrocortisone/HP-β-CyD nanofibrous webs showed different released profiles for the same sample amount (~40 mg) of webs and this reflects the different hydrocortisone contents in hydrocortisone/HP-β-CyD nanofibers. When the released concentration of hydrocortisone is compared with the theoretical/initial concentrations, it is noticed that ~80%, ~86% and ~90% of hydrocortisone is released from the hydrocortisone/HP-β-CyD (1/1), hydrocortisone/HP-β-CyD (1/1.5) and hydrocortisone/HP-β-CyD (1/2) nanofibrous webs, respectively. As is seen, hydrocortisone/HP-β-CyD (1/2) nanofibers indicated the highest initial release amount of hydrocortisone compared to the other two hydrocortisone/HP-β-CyD (1/1 and 1/1.5) nanofibers. This is most probably due to the fully amorphous state of hydrocortisone in the hydrocortisone/HP-β-CyD (1/2) nanofibrous web, which ensures a superior dissolution and release profile in the aqueous medium. On the other hand, the presence of some uncomplexed hydrocortisone in hydrocortisone/HP-β-CyD (1/1 and 1/1.5) nanofibrous webs leads to a lower dissolution and released amount of hydrocortisone in the given time period. In brief, both the inclusion complexation and the nanofibrous structure of the hydrocortisone/HP-β-CyD nanofibers enhanced the dissolution rate and the release of hydrocortisone, which suggests that hydrocortisone/HP-β-CyD nanofibrous webs may have huge potential to be utilized as a fast-dissolving oral drug delivery system.

The solubility improvement of hydrocortisone in hydrocortisone/HP-β-CyD (1/1, 1/1.5 and 1/2) nanofibers was also demonstrated by the constant stirring in water for 24 hours at room temperature. Firstly, hydrocortisone and hydrocortisone/HP-β-CyD (1/1, 1/1.5 and 1/2) nanofibers having the same amount of hydrocortisone were dissolved in water. Then, the solutions were filtered to remove the undissolved fractions of hydrocortisone and UV-vis spectroscopy measurements were carried out for the ultimate aqueous solutions. The UV-vis spectra of the solution of hydrocortisone and hydrocortisone/HP-β-CyD nanofibers are shown in Fig. 8c. Even though all solutions were prepared with the same amount of hydrocortisone (2.2 mM), the intensities of the hydrocortisone/HP-β-CyD nanofiber solutions are higher than that of the hydrocortisone solution. This finding clearly indicated that the inclusion complexation enhanced the water solubility of hydrocortisone in hydrocortisone/HP-β-CyD nanofibers. Actually, hydrocortisone/HP-β-CyD (1/1) nanofibers (~20 mg), hydrocortisone/HP-β-CyD (1/1.5) nanofibers (~28 mg) and hydrocortisone/HP-β-CyD (1/2) nanofibers (~35 mg) were weighed so as to have the same amount of hydrocortisone. As seen from the UV-vis spectra, hydrocortisone/HP-β-CyD (1/1) nanofibers depict a bit lower intensity compared to hydrocortisone/HP-β-CyD (1/1.5 and 1/2) nanofibers. Even though there is a high amount of uncomplexed and crystalline hydrocortisone in hydrocortisone/HP-β-CyD (1/1) nanofibers (which was proved by the XRD and DSC analyses), the dissolution of hydrocortisone/HP-β-CyD (1/1) nanofibers in high water content (5 mL) and the long stirring period of 24 hours achieve dissolution of crystalline hydrocortisone in the presence of HP-β-CyD, so the intensity of the UV-vis spectrum is not very different from those of hydrocortisone/HP-β-CyD (1/1.5 and 1/2) nanofibers. Yet, there were still little amounts of uncomplexed/crystalline hydrocortisone in the solution of hydrocortisone/HP-β-CyD (1/1) nanofibers which could not be dissolved and filtered out, so the intensity of the UV-vis spectrum is a bit lower than those of the solution of hydrocortisone/HP-β-CyD (1/1.5 and 1/2) nanofibers. On the other hand, the UV-vis spectrum of hydrocortisone/HP-β-CyD (1/1.5) nanofibers depicted almost the same intensity as the UV-vis spectrum of hydrocortisone/HP-β-CyD (1/2) nanofibers, since the experimental conditions provided enough time for some uncomplexed hydrocortisone to form inclusion complexes

with free HP-β-CyD molecules in this highly diluted solution. For the electrospinning solution of hydrocortisone/HP-β-CyD (1/1 and 1/1.5), the highly viscous solution of HP-β-CyD having a very high concentration (180%, w/v) makes stirring and mixing of the system difficult to achieve efficient inclusion complexation between hydrocortisone and HP-β-CyD. Therefore, a lower complexation efficiency was obtained in the case of the hydrocortisone/HP-β-CyD (1/1 and 1/1.5) systems compared to the hydrocortisone/HP-β-CyD (1/2) system. The inclusion complexation between hydrocortisone and HP-β-CyD was much more efficient and hydrocortisone was fully complexed in the hydrocortisone/HP-β-CyD (1/2) system due to the higher content of HP-β-CyD. In addition, a very similar UV-vis spectrum (Fig. S2†) was recorded for the hydrocortisone/HP-β-CyD (1/2) complex nanofibers stored for 3 months (55–65% RH and ~22 °C) confirming the stability of the hydrocortisone/HP-β-CyD nanofibers over long storage periods.

The fast dissolution of hydrocortisone/HP-β-CyD nanofibrous webs (~6 mg) was visually examined by immersing the nanofibrous webs in 4 mL of water in Petri dishes (Fig. 9 and Video S1†). The hydrocortisone powder (~1.2 mg) was also tested for comparison. Here, hydrocortisone/HP-β-CyD nanofibrous webs immediately dissolved upon contact with water; in contrast, the pure hydrocortisone powder remained on the water surface over this period of time without dissolution showing that it is a poorly water-soluble drug (Fig. 9). The dissolution test also proved the existence of uncomplexed hydrocortisone in the hydrocortisone/HP-β-CyD (1/1 and 1/1.5) nanofibrous webs. As seen in Fig. 9, while hydrocortisone/HP-β-CyD (1/2) nanofibers completely dissolved in water in 2 seconds, there are still undissolved hydrocortisone fractions in hydrocortisone/HP-β-CyD (1/1 and 1/1.5) solutions because of the uncomplexed/crystalline hydrocortisone content in the hydrocortisone/HP-β-CyD (1/1 and 1/1.5) nanofibrous webs. Since the hydrocortisone/HP-β-CyD (1/1) nanofibrous web contains a higher amount of uncomplexed hydrocortisone compared to the hydrocortisone/HP-β-CyD (1/1.5) nanofibrous web, the undissolved hydrocortisone fractions are more obvious in the Petri dish in the case of hydrocortisone/HP-β-CyD (1/1) nanofibers. Even so, a fast-dissolving character was observed for the hydrocortisone/HP-β-CyD (1/2) nanofibrous web resulting in complete dissolution and clear solution without any indication of undissolved hydrocortisone.

The disintegration of hydrocortisone/HP-β-CyD nanofibrous webs was further examined using wet filter paper to simulate the moist environment of the oral cavity.[58] As observed in Fig. 10 and Video S2,† the hydrocortisone/HP-β-CyD (1/2) nanofibrous web was quickly adsorbed by artificial saliva and dissolved instantly. On the other hand, the hydrocortisone/HP-β-CyD (1/1) nanofibrous web indicated a slower disintegration profile compared to the hydrocortisone/HP-β-CyD (1/2) nanofibrous web because of the uncomplexed/crystalline hydrocortisone content. The Hydrocortisone/HP-β-CyD (1/1.5) nanofibrous web indicated an intermediate performance among the others, because of the small uncomplexed

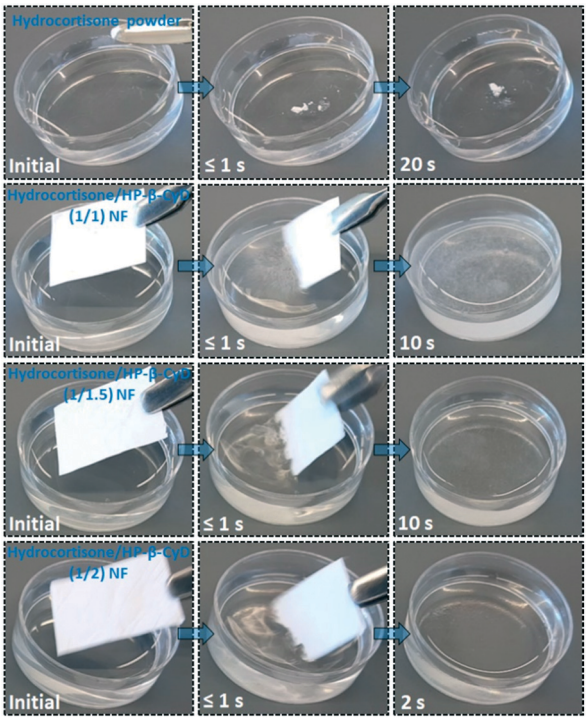

Fig. 9 The dissolution behaviour of hydrocortisone powder and hydrocortisone/HP-β-CyD (1/1, 1/1.5 and 1/2) nanofibrous webs in distilled water. The pictures were captured from the video given as Video S1.†

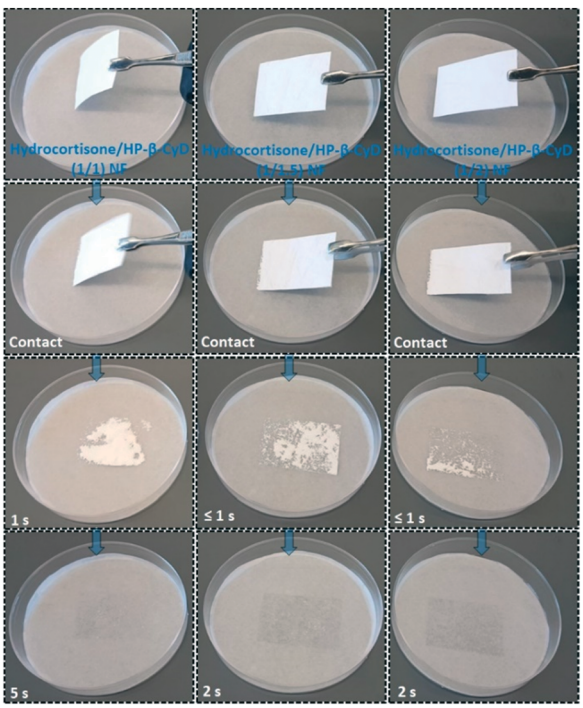

Fig. 10 The disintegration behaviour of hydrocortisone/HP-β-CyD (1/1), hydrocortisone/HP-β-CyD (1/1.5) and hydrocortisone/HP-β-CyD (1/2) nanofibrous webs in an artificial saliva environment. The pictures were captured from the video given as Video S2.†

hydrocortisone content in it. The high water solubility of HP-β-CyD is a significant dynamic factor for the high dissolution and disintegration rates of the hydrocortisone/HP-β-CyD nanofibrous webs.[40] Furthermore, the porous structure and high surface area of the nanofibrous webs ensure an incredible penetration path and interaction sites for the aqueous system through the nanofibers which also provide fast disintegration and dissolution of nanofibers.[21] To conclude, the nanoporous structure of hydrocortisone/HP-β-CyD nanofibrous webs can lead to their easy penetration to saliva in the mouth and high water solubility of HP-β-CyD and inclusion complexation of hydrocortisone with HP-β-CyD can provide fast-dissolution and instant release of hydrocortisone which makes hydrocortisone/HP-β-CyD nanofibrous webs very appropriate for fast-dissolving oral drug delivery systems.

Conclusion

Electrospun nanofibrous webs from inclusion complexes of drug/cyclodextrin systems can be very promising materials for the development of fast-dissolving oral drug delivery systems. Cyclodextrins are already well-known and applicable in pharmaceutics due to their solubility enhancement of poorly water-soluble drugs by forming inclusion complexation with a variety of drug molecules. Therefore, the choice of cyclodextrins as nanofiber matrices and encapsulating drug molecules within cyclodextrin cavities by inclusion complexation would enhance the water solubility and fast-dissolution of poorly water-soluble drugs for oral drug delivery systems. For this purpose, we have produced hydrocortisone/HP-β-CyD nanofibrous webs by electrospinning. The initial molar ratios of hydrocortisone/HP-β-CyD (1/1, 1/1.5 and 1/2) in aqueous solutions were completely preserved yielding hydrocortisone/HP-β-CyD nanofibers having the same molar ratios confirming that the electrospinning process was quite efficient without any loss of hydrocortisone. The electrospinning of hydrocortisone/HP-β-CyD aqueous solutions yielded defect-free nanofibers which were collected in the form of self-standing and flexible nanofibrous webs. The electrospun hydrocortisone/HP-β-CyD nanofibrous webs were readily dissolved when placed in water or when wetted with artificial saliva. The results elucidated that electrospun hydrocortisone/HP-β-CyD nanofibrous webs could be promising materials as fast-dissolving oral drug delivery systems. In conclusion, cyclodextrins form inclusion complexes with a variety of drugs; hence, this proof-of-concept study dealing with electrospun hydrocortisone/HP-β-CyD nanofibrous webs can be extended to other drug/CyD inclusion complex nanofibers in order to develop fast-dissolving oral drug delivery systems.

Author contributions

T. U. and A. C. designed the study. A. C. performed the experimental studies. A. C. and T. U. wrote the manuscript and have given approval to the final version of the manuscript.

Conflicts of interest

There are no conflicts to declare of interest.

Acknowledgements

This work made use of the Cornell Center for Materials Research Shared Facilities, which are supported through the NSF MRSEC program (DMR-1719875), the Cornell Chemistry NMR Facility supported in part by the NSF MRI program (CHE-1531632), and the Department of Fiber Science & Apparel Design facilities. Prof. Uyar acknowledges the start-up funding from the College of Human Ecology at Cornell University. The partial funding for this research was also graciously provided by Nixon Family (Lea and John Nixon) thru College of Human Ecology at Cornell University.

References

1 A. C. Liang and L. H. Chen, *Expert Opin. Ther. Pat.*, 2001, **11**, 981–986.
2 R. Bala, S. Khanna, P. Pawar and S. Arora, *Int. J. Pharm. Invest.*, 2013, **3**, 67.
3 V. A. Saharan, *Current Advances in Drug Delivery Through Fast Dissolving/Disintegrating Dosage Forms*, Bentham Science Publishers, Sharjah, 2017.
4 R. S. Kumar and T. N. S. Yagnesh, *Indo Am. J. Pharm. Res.*, 2018, **8**, 1464–1472.
5 R. Rahane and P. R. Rachh, *J. Drug Delivery Ther.*, 2018, **8**, 50–55.
6 R. P. Dixit and S. P. Puthli, *J. Controlled Release*, 2009, **139**, 94–107.
7 T. Nagaraju, R. Gowthami, M. Rajashekar, S. Sandeep, M. Mallesham, D. Sathish and Y. K. Shravan, *Curr. Drug Delivery*, 2013, **10**, 96–108.
8 Z. I. Yildiz, A. Celebioglu and T. Uyar, *Int. J. Pharm.*, 2017, **531**, 550–558.
9 X. Li, L. Lin, Y. Zhu, W. Liu, T. Yu and M. Ge, *Polym. Compos.*, 2013, **34**, 282–287.
10 X. Li, M. A. Kanjwal, L. Lin and I. S. Chronakis, *Colloids Surf., B*, 2013, **103**, 182–188.
11 X.-Y. Li, Y.-C. Li, D.-G. Yu, Y.-Z. Liao and X. Wang, *Int. J. Mol. Sci.*, 2013, **14**, 21647–21659.
12 J. L. Manasco, C. Tang, N. A. Burns, C. D. Saquing and S. A. Khan, *RSC Adv.*, 2014, **4**, 13274.
13 U. E. Illangakoon, H. Gill, G. C. Shearman, M. Parhizkar, S. Mahalingam, N. P. Chatterton and G. R. Williams, *Int. J. Pharm.*, 2014, **477**, 369–379.
14 Z. I. Yildiz and T. Uyar, *Appl. Surf. Sci.*, 2019, **492**, 626–633.
15 A. Balogh, T. Horváthová, Z. Fülöp, T. Loftsson, A. H. Harasztos, G. Marosi and Z. K. Nagy, *J. Drug Delivery Sci. Technol.*, 2015, **26**, 28–34.
16 H. W. Kwak, H. Woo, I.-C. Kim and K. H. Lee, *RSC Adv.*, 2017, **7**, 40411–40417.
17 D.-G. Yu, X.-X. Shen, C. Branford-White, K. White, L.-M. Zhu and S. W. Annie Bligh, *Nanotechnology*, 2009, **20**, 055104.
18 J.-J. Li, Y.-Y. Yang, D.-G. Yu, Q. Du and X.-L. Yang, *Eur. J. Pharm. Sci.*, 2018, **122**, 195–204.

19 Z. Aytac, S. Ipek, I. Erol, E. Durgun and T. Uyar, *Colloids Surf., B*, 2019, **178**, 129–136.
20 Y.-H. Wu, D.-G. Yu, X.-Y. Li, A.-H. Diao, U. E. Illangakoon and G. R. Williams, *J. Mater. Sci.*, 2015, **50**, 3604–3613.
21 D. G. Yu, J. J. Li, G. R. Williams and M. Zhao, *J. Controlled Release*, 2018, **292**, 91–110.
22 P. Vass, B. Démuth, A. Farkas, E. Hirsch, E. Szabó, B. Nagy, S. K. Andersen, T. Vigh, G. Verreck, I. Csontos, G. Marosi and Z. K. Nagy, *J. Controlled Release*, 2019, **298**, 120–127.
23 A. Balogh, *et al.*, *Chem. Eng. J.*, 2018, **350**, 290–299.
24 A. Domokos, *et al.*, *Eur. J. Pharmacol.*, 2019, **130**, 91–99.
25 Z. K. Nagy, A. Balogh, G. Drávavölgyi, J. Ferguson, H. Pataki, B. Vajna and G. Marosi, *J. Pharm. Sci.*, 2013, **102**, 508–517.
26 A. Balogh, B. Farkas, K. Faragó, A. Farkas, I. Wagner, G. Verreck and G. Marosi, *J. Pharm. Sci.*, 2015, **104**, 1767–1776.
27 H. Jianxin and Z. Yuman, *Electrospinning: Nanofabrication and Applications, Multineedle Electrospinning*, Micro and Nano Technologies, William Andrew, 2019, pp. 201–218.
28 Z. Aytac and T. Uyar, *Int. J. Pharm.*, 2017, **518**, 177–184.
29 L. Vysloužilová, M. Buzgo, P. Pokorný, J. Chvojka, A. Míčková, M. Rampichová, J. Kula, K. Pejchar, M. Bílek, D. Lukáš and E. Amler, *Int. J. Pharm.*, 2017, **516**, 293–300.
30 J. Quan, Y. Yu, C. Branford-White, G. R. Williams, D.-G. Yu, W. Nie and L.-M. Zhu, *Colloids Surf., B*, 2011, **88**, 304–309.
31 H. Bukhary, G. R. Williams and M. Orlu, *Int. J. Pharm.*, 2018, **549**, 446–455.
32 F. Mano, M. Martins, I. Sá-Nogueira, S. Barreiros, J. P. Borges, R. L. Reis, A. R. C. Duarte and A. Paiva, *AAPS PharmSciTech*, 2017, **18**, 2579–2585.
33 S. Nam, J.-J. Lee, S. Y. Lee, J. Y. Jeong, W.-S. Kang and H.-J. Cho, *Int. J. Pharm.*, 2017, **526**, 225–234.
34 Z. Qin, X.-W. Jia, Q. Liu, B. Kong and H. Wang, *Int. J. Biol. Macromol.*, 2019, **137**, 224–231.
35 D.-G. Yu, J.-J. Li, G. R. Williams and M. Zhao, *J. Controlled Release*, 2018, **292**, 91–110.
36 T. Vigh, T. Horváthová, A. Balogh, P. L. Sóti, G. Drávavölgyi, Z. K. Nagy and G. Marosi, *Eur. J. Pharm. Sci.*, 2013, **49**, 595–602.
37 A. Celebioglu and T. Uyar, *Mol. Pharmaceutics*, 2019, **16**, 4387–4398.
38 *Cyclodextrins in Pharmaceutics, Cosmetics, and Biomedicine: Current and Future Industrial Applications*, ed. E. Bilensoy, John Wiley & Sons, Inc., Hoboken, NJ, USA, 2011.
39 S. Carneiro, F. Costa Duarte, L. Heimfarth, J. Siqueira Quintans, L. Quintans-Júnior, V. Veiga Júnior and Á. Neves de Lima, *Int. J. Mol. Sci.*, 2019, **20**, 642.
40 T. Loftsson and M. E. Brewster, *J. Pharm. Pharmacol.*, 2010, **62**, 1607–1621.
41 L. Szente, *Adv. Drug Delivery Rev.*, 1999, **36**, 17–28.
42 P. Saokham, C. Muankaew, P. Jansook and T. Loftsson, *Molecules*, 2018, **23**, 1161.
43 F. Topuz and T. Uyar, *Pharmaceutics*, 2019, **11**, 1–35.
44 Y. Lee, K. Kim, M. Kim, D. H. Choi and S. H. Jeong, *J. Pharm. Invest.*, 2017, **47**, 183–201.
45 A. Shahiwala, *Expert Opin. Drug Delivery*, 2011, **8**, 1521–1529.
46 C. Schönbeck, T. L. Madsen, G. H. Peters, R. Holm and T. Loftsson, *Int. J. Pharm.*, 2017, **531**, 504–511.
47 D. H. Schwarz, A. Engelke and G. Wenz, *Int. J. Pharm.*, 2017, **531**, 559–567.
48 M. Orlu-Gul, G. Fisco, D. Parmar, H. Gill and C. Tuleu, *Drug Dev. Ind. Pharm.*, 2013, **39**, 1028–1036.
49 T. Loftsson and M. E. Brewster, *J. Pharm. Pharmacol.*, 2011, **63**, 1119–1135.
50 T. Kristmundsdóttir, T. Loftsson and W. P. Holbrook, *Int. J. Pharm.*, 1996, **139**, 63–68.
51 A. Bary, *Eur. J. Pharm. Biopharm.*, 2000, **50**, 237–244.
52 A. Hemati Azandaryani, K. Derakhshandeh and E. Arkan, *Int. J. Polym. Mater. Polym. Biomater.*, 2018, **67**, 677–685.
53 Y. Fazli, Z. Shariatinia, I. Kohsari, A. Azadmehr and S. M. Pourmortazavi, *Int. J. Pharm.*, 2016, **513**, 636–647.
54 P. Peh, N. S. J. Lim, A. Blocki, S. M. L. Chee, H. C. Park, S. Liao, C. Chan and M. Raghunath, *Bioconjugate Chem.*, 2015, **26**, 1348–1358.
55 G. Jin, M. P. Prabhakaran, D. Kai and S. Ramakrishna, *Eur. J. Pharm. Biopharm.*, 2013, **85**, 689–698.
56 R. Elia, D. R. Newhide, P. D. Pedevillano, G. R. Reiss, M. A. Firpo, E. W. Hsu, D. L. Kaplan, G. D. Prestwich and R. A. Peattie, *J. Biomater. Appl.*, 2013, **27**, 749–762.
57 T. Higuchi and K. A. Connors, *Adv. Anal. Chem. Instrum.*, 1965, **4**, 117–212.
58 Y. Bi, H. Sunada, Y. Yonezawa, K. Danjo, A. Otsuka and K. IIDA, *Chem. Pharm. Bull.*, 1996, **44**, 2121–2127.
59 Z. K. Nagy, A. Balogh, B. Démuth, H. Pataki, T. Vigh, B. Szabó, K. Molnár, B. T. Schmidt, P. Horák, G. Marosi, G. Verreck, I. Van Assche and M. E. Brewster, *Int. J. Pharm.*, 2015, **480**, 137–142.
60 J. H. Wendorff, S. Agarwal and A. Greiner, *Electrospinning: Materials, Processing, and Applications*, Wiley-VCH Verlag GmbH & Co. KGaA, Weinheim, Germany, 2012.
61 T. Uyar and F. Besenbacher, *Polymer*, 2008, **49**, 5336–5343.
62 P. Mura, *J. Pharm. Biomed. Anal.*, 2015, **113**, 226–238.
63 G. Narayanan, R. Boy, B. S. Gupta and A. E. Tonelli, *Polym. Test.*, 2017, **62**, 402–439.
64 Z. Hussain, H. Katas, M. C. I. M. Amin, E. Kumolosasi, F. Buang and S. Sahudin, *Int. J. Pharm.*, 2013, **444**, 109–119.
65 D. G. Yu, J. M. Yang, C. Branford-White, P. Lu, L. Zhang and L. M. Zhu, *Int. J. Pharm.*, 2010, **400**, 158–164.
66 A. Celebioglu and T. Uyar, *Nanoscale*, 2012, **4**, 621–631.
67 N. G. Hădărugă, G. N. Bandur, I. David and D. I. Hădărugă, *Environ. Chem. Lett.*, 2019, **17**, 349–373.
68 M. E. Brewster and T. Loftsson, *Adv. Drug Delivery Rev.*, 2007, **59**, 645–666.
69 H. M. C. Marques, *Flavour Fragrance J.*, 2010, **25**, 313–326.
70 N. M. Davies, G. Wang and I. G. Tucker, *Int. J. Pharm.*, 1997, **156**, 201–209.
71 T. Loftsson, M. Másson and H. H. Sigurdsson, *Int. J. Pharm.*, 2002, **232**, 35–43.
72 M. Messner, S. V. Kurkov, M. E. Brewster, P. Jansook and T. Loftsson, *Int. J. Pharm.*, 2011, **407**, 174–183.
73 T. Loftsson, D. Hreinsdóttir and M. Másson, *Int. J. Pharm.*, 2005, **302**, 18–28.
74 T. Loftsson, H. Frikdriksdóttir, A. M. Sigurkdardóttir and H. Ueda, *Int. J. Pharm.*, 1994, **110**, 169–177.

